

## Chapter 4

### Validation

Large-eddy simulations of turbulent canonical test cases are presented in this chapter for validation purposes. In the cases presented, high-fidelity turbulent DNS results are used as the “gold” standard for measuring the accuracy of our models. DNS is recognized in the community as providing the highest level of turbulent description due to its model-free approach and resolution of the entire scales of motion. Thus, DNS is a reliable computational tool which complements the time trusted methodology of experimental research. The dynamic Smagorinsky LES models, described in detail in Chapter 2, for momentum and scalar transfer are utilized and their results are compared. The first test case corresponds to the classical incompressible turbulent channel configuration. This flow corresponds to a planar, fully developed flow where turbulence develops and sustains itself to form wall-bounded turbulent structures. This configuration has been studied by various researchers for fundamental turbulent validation studies, visualization and modeling purposes. The second test corresponds to a similar configuration but with the new complexity of strong temperature gradients at the wall. This adds to the richness of the turbulent physics since it brings in low-Mach number transport equations in a variable density framework. Results are compared to the DNS data from Nicoud et al.

In general, the systematic process of validation has been described as using the right models for a particular study, often quoted as: *“The process of determining the degree to which a model is an accurate representation of the real world from the perspective of the intended uses of the model”* [1]. Validation examines if the conceptual models, computational models as implemented into

the CFD code and computational simulation agree with real world observations. The strategy is to identify and quantify error and uncertainty through comparison of simulation results with experimental data. The experiment data sets themselves will contain bias errors and random errors which must be properly quantified and documented as part of the data set. The accuracy required in the validation activities is dependent on the application, and so, the validation should be flexible to allow various levels of accuracy. Systematic validation reports have been studied for CFD solvers in industry or national laboratory applications. An example of this is the Fire Dynamic Simulator from NIST which presents extensive validation suites (test cases) with comparison to real-world test studies and experimental results. Another laboratory that presents a systematic approach to validation is Sandia National Laboratories verification and validation report where they quantify validation errors and uncertainties with experiments. Our focus in this proposal is to apply a simple qualitative verification procedure where expert model data is compared to high-fidelity real world results.

## 4.1 Turbulence in channel flow

A classical turbulent benchmark case used to study the mechanics of wall-bounded turbulent flows is the Kim, Moser and Moin configuration originally presented in a landmark paper [1] and extensively referred to in this proposal. This work presents a direct numerical simulation of plane turbulent channel flow where all essential scales of motion are resolved. This provides us with a valuable database for quantitative and qualitative studies of turbulent structure in wall bounded flows and for validation of turbulence closure models.

### 4.1.1 Wall bounded terminology and resolution requirements

In near wall turbulent flows the viscosity and the wall shear stress are important parameters. Normally a model for the turbulent structure is proposed which consists of two distinct regions, a viscous sublayer and an outer region (log region). The difference in the regions lies in their contributions to the total shear stress profile  $\frac{\tau}{\rho} = (\nu + \nu_t)\partial u/\partial y$  where for the viscous sublayer  $\nu > \nu_t$  and for the outer region  $\nu < \nu_t$ . Viscous scales are normally defined based on these quantities for appropriate velocity-scales and length-scales close to the wall. The friction velocity,  $u_\tau = \sqrt{\tau_{wall}/\rho}$ , and the viscous length scale  $\delta_v = \nu/u_{tau}$  are used to define the friction Reynolds number as  $Re_\tau = \frac{u_{tau}\delta}{\nu} = \frac{\delta}{\delta_v}$  where  $\delta$  is the channel half-height,  $\delta = 1$ . The distance from the wall in viscous lengths is defined by  $y^+ = \frac{u_\tau y}{\nu}$ , also called wall-units, where by inspection we can see that the role of wall-units is similar to a measure of the local Reynolds number. Lateral velocity and pressure can also be defined in wall units, in summary:

$$u^+ = \frac{u}{u_\tau} = \frac{u}{\sqrt{\frac{\tau_{wall}}{\rho}}} = \frac{u_{inf}}{\sqrt{\frac{C_f}{2}}}, y^+ = \frac{y u_\tau}{\nu} = \frac{y \sqrt{\frac{\tau_{wall}}{\rho}}}{\nu} = \frac{y u_{inf} \sqrt{\frac{C_f}{2}}}{\nu}$$

$$v^+ = \frac{v}{u_\tau} = \frac{v}{\sqrt{\frac{\tau_{wall}}{\rho}}} = \frac{v_{inf}}{\sqrt{\frac{C_f}{2}}}, p^+ = \frac{\mu \frac{dP}{dx}}{\left( \rho^{\frac{1}{2}} \tau_{wall}^{\frac{3}{2}} \right)}$$

In principle the above normalizations have been used to obtain a universal law of the wall for the viscous sublayer and the outer region (log-region). This is done through integration of the normalized total shear profiles and invoking the classical Prandlt mixing length hypothesis. The results are the law of wall valid for turbulent boundary layers and channel flows for the case of negligible streamwise pressure gradient.

Law of the wall which states that in the viscous sublayer region ( $y^+ < 5$ )

$$u^+ = y^+$$

And in the log-law region ( $y^+ > 30$ )

$$u^+ = \frac{1}{K} \ln(y^+) + B$$

where  $K = 0.41$  is the Von Karman constant and  $B = 5.2$  is a turbulent constant.

Wall bounded Large-eddy simulations have stringent resolution requirements, similar to DNS, near the wall. This is necessary for it to capture the wall-layer structures that arise when a solid boundary is present. This type of technique is called a “resolved” Large-eddy simulation. When designing a turbulent grid for this configuration, one of the interests will be to spatially resolve the viscous region, log region and the inner layer eddies. In the outer layer, the important

eddies will scale with boundary layer thickness or characteristic length-scale, like the channel half-height  $\delta$ , and its resolution should be of order  $\delta$ . The resolution of the inner-layer is much more demanding since its dynamics are dominated by sweeping and ejecting processes that are generated by the presence (and destruction) of quasi-streamwise vortices. The dimensions of these vortices are constant when normalized in wall-units. Therefore, to resolve the sublayer constant grid spacing in wall units must be used [ref Piomelli]. For channel flows this requirement results in streamwise and spanwise grid sizes of:  $\Delta x^+ \cong 100, \Delta z^+ \cong 20$  for spectral methods and half of that for low order finite-difference solvers  $\Delta x^+ \cong 50, \Delta z^+ \cong 15$  as suggested by Piomelli []. Effective grid design is achieved through hyperbolic stretching of the normal distance component, clustering the grids in regions of high activity and using coarser resolution in the outer region.

## 4.1.2 Computational domain

Fully developed plane channel flow is homogeneous in the streamwise (x) and spanwise directions (z) and periodic boundary conditions can be used in these coordinates. The use of periodicity in the homogenous direction is valid as long as the relevant computational dimension is chosen to include the largest eddy in the flow. The periodic domain sizes were originally selected by Kim et al, so that the two point correlations in x and z would be near zero at half the domain size. The pressure gradient that drives the flows is adjusted at every time step to impose a constant mass flux through the channel. This is based on the following conservation equation,

$$\left(\frac{dP}{dx}\right)^n = \left(\frac{dP}{dx}\right)^{n+1} - 2\left(\frac{\dot{m}^{*n} - \dot{m}}{dt}\right) - 2\left(\frac{\dot{m}^{*n-1} - \dot{m}}{dt}\right) \text{ where } \dot{m}^{*n} \text{ is the calculated mass flux at the}$$

current time level and  $\dot{m}$  is the required mass flux. The computation is performed using the LES Dynamic Eddy Viscosity model with ~200,00 grid points (48, 65, 64 in x, y, z) with a frictional Reynolds number of 395, based on the frictional velocity and channel half-height. A classical Smagorinsky type model, as presented in section 2, is utilized to provide the relationship between the rate of strain, dynamic coefficient with the shear stress. The minimization technique of Lily et al is used to solve for the dynamic coefficient as presented in table1. The streamwise and spanwise computational periods are chosen to be  $2\pi$  and  $\pi$  respectively with the channel half-height defined as  $\delta = 1$ . With this computational domain, the grid spacing in the streamwise and spanwise directions are respectively  $\Delta x^+ = 50$  and  $\Delta z^+ = 15$  in wall units. A non-uniform mesh is used in the wall-normal direction where the first point away from the wall is  $y^+ \cong 1$  and the maximum spacing at the center of the channel is  $y^+ \cong 15$ .

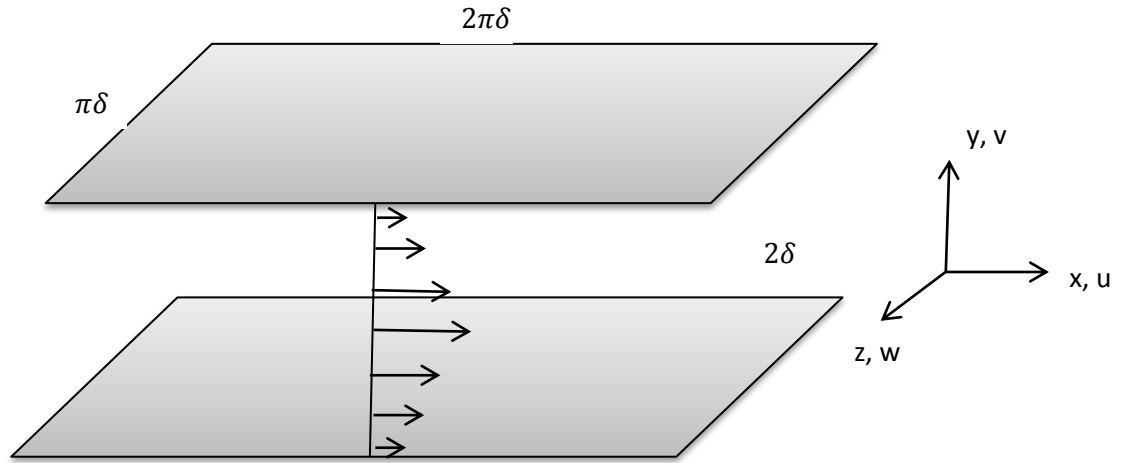


Figure 1. Turbulent Channel Schematic,  $Re_\tau = 395$ .

$(L_x L_y L_z)^*$	$(n_x n_y n_z)$	<i>grid stretching</i>
$(2\pi\delta, 2\delta, \pi)$	$(48, 65, 64)$	<ul style="list-style-type: none"> <li>- Wall-normal hyperbolic (<math>\alpha = 2.75</math>)</li> <li>- Uniform grid in x, z</li> </ul>
<i>Resolution criteria</i> (finite differences)	<i>Turbulence model</i>	<b>Turbulent coefficient</b> <b>Minimization technique (Lily, et al)</b>
$\Delta x^+ \cong 50$ $\Delta z^+ \cong 15$ $y^+ \cong 1$	LES Dynamic eddy viscosity (Smagorinsky type model)	$C_{ev}(x, y, z, t) = -\frac{1}{2} \frac{\langle L_{ij} M_{ij} \rangle_{avg}}{\langle M_{ij} M_{ij} \rangle_{avg}}$
$Re_{bulk} = 6900$ $Re_\tau = 395$		<b>Averaging type:</b> Lagrangian Planar (option) Line (option)
<i>wall boundary</i>	<i>Mass flux option</i>	<i>Periodicity</i>
$u_{iwall} = No\ slip$ $T_{wall} = 300K$	Adjust pressure gradient to maintain constant mass flux	Streamwise, Spanwise

### 4.1.3 Results

The computational study is performed closely following the parameter table presented in the previous section on Table 1. Initial conditions in the channel are specified with random noise having a magnitude of 40% serving as a kick-start for channel flow instabilities. The flow field variables are integrated forward in time until the flow reaches a statistically steady state. The steady state can be identified by a linear profile of the total shear stress  $-\overline{u'v'} + \nu\partial\bar{u}/\partial y$  and by a quasi-periodic (steady) total kinetic energy. The fluctuations of turbulent kinetic energy serve as a good monitor for the total energy variations of the channel. Thus, the simulation total run time has to include the development of a steady turbulent kinetic energy history plus several time scales designated Large-eddy turn over time (LETOT),  $LETOT \sim \frac{\delta}{u_\tau}$ . A total of 10 LETOTS were used in this study with 5 measurements taken per time-scale. Thus, the post-processing of the random fields  $U_i(x, t)$  is done by performing a temporal running average and a spatial average over horizontal planes in the homogeneous directions to obtain the various statistical correlations.

Profiles of mean velocity non-dimensionalized by the wall shear velocity is shown in figure 1. Also shown in the figure is the mean velocity profile from the DNS results from Kim, Moser and Moin (ref). The dashed lines represent the law of the wall and the log law. Within the viscous sublayer,  $y^+ < 5$ , both results follow the linear law of the wall. Similarly in the log-layer,  $y^+ > 10$  simulation results show good comparison to the log-law and to the DNS data except for the wake region ( $y^+ > 200$ ) where the peak differences are less than 2 percent.



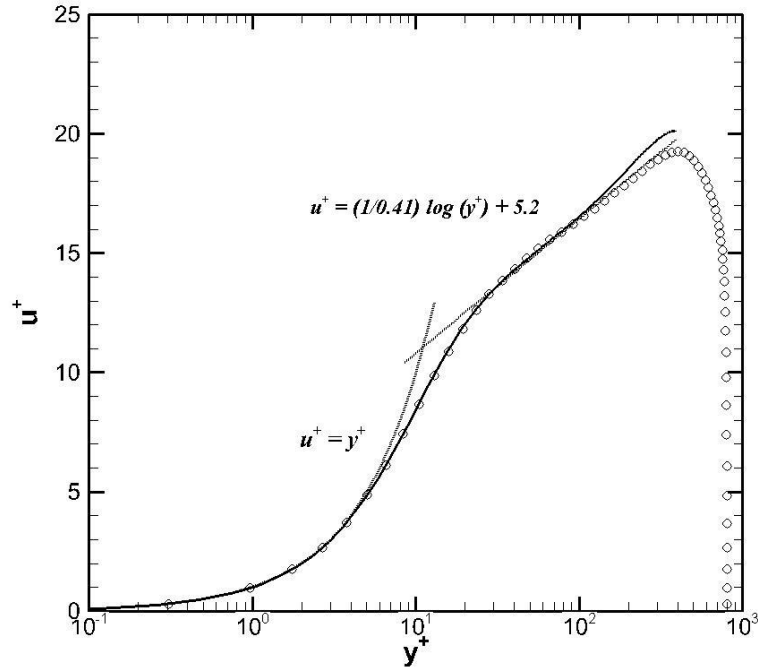


Figure 2. Mean velocity profiles  $Re_\tau = 395$ . o—are current LES simulations and, --- solid black line is reference DNS data.

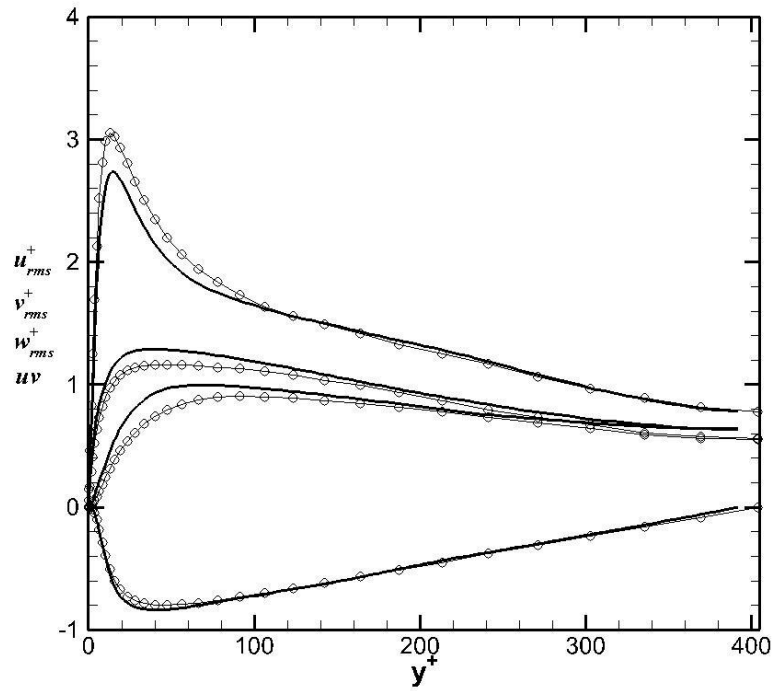
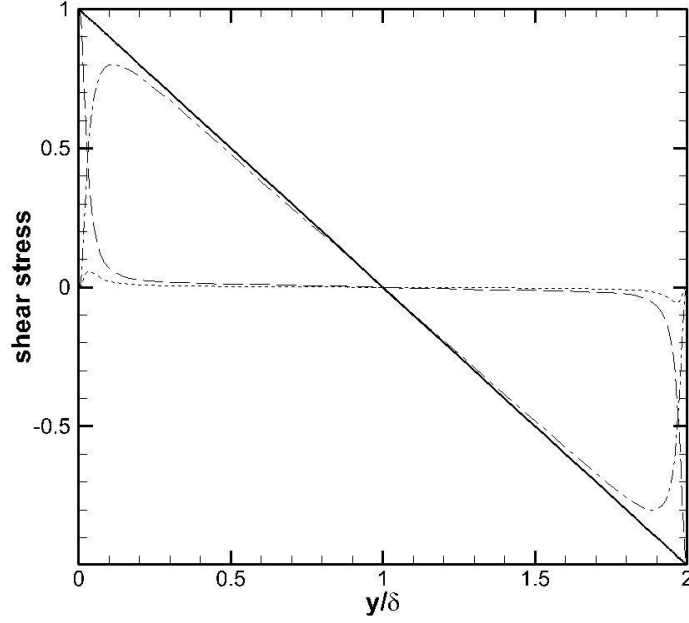


Figure 3. Turbulent intensities of velocity fluctuation normalized by wall shear velocity,  $Re_\tau = 395$ . o—are current LES simulations and, --- solid black line is reference DNS data.

Turbulent intensities normalized by the frictional velocities are shown in figure 3 and they are compared with DNS results at Reynolds number  $Re_\tau = 400$ . This is shown up to the centerline of the channel since the profiles are symmetrical. The symmetry of the profiles also shows the adequacy of the sample taken for the average. Although the shape of the profiles agree very well in the wake and log-region, one can still see differences below  $y^+ \sim 150$  and in particular below the viscous wall region  $y^+ < 50$ . The modeling of the viscous region is a complex task due since it contains the most rigorous turbulent activity. The production, dissipation, turbulent kinetic energy and anisotropy all achieve their peak values at  $y^+ < 20$  for flows at high Reynolds numbers (pope). It is due to these phenomena that the modeling errors are most evident in this region. Also shown in figure 3 are comparisons of the Reynolds stress,  $uv$ . Similar to the intensity profiles, the wake and outer region provides the best comparison to the actual turbulence physics. The Reynolds shear stress and its constituents are plotted in figure 4. Due to mechanical conservation of energy and statistical convergence we should expect the total shear stress to be linear across the channel. The behavior of the total shear stress in the vicinity of a wall for a fully developed channel flow can be deduced from the following equation,

$$-\frac{\overline{u'v'}}{u_\tau^2} + \frac{\overline{2\nu_{sgs}S_{ij}}}{u_\tau^2} + \frac{du^+}{dy^+} = 1 - \frac{y^+}{\delta^+}$$

Where the components are: the resolved Reynolds stress, modeled stress and viscous stress, respectively. The linearity of the conservation property will hold true once we add the total shear constituents. One subtlety encountered in this analysis is the modeled stress post-processing handling must include the product of the eddy viscosity and rate of strain inside the averaging operator due to its spatial and temporal variations in the flow.



**Figure 4. Reynolds shear stress normalized by friction velocity,  $Re_\tau = 400$ . Represents the resolved stress, modeled stress and the viscous stress.**

Visualization of the flow field is shown on figures 5-6. Figure 5 presents three dimensional contours of the velocity field showing an instantaneous representation of the turbulent field. To obtain a better representation of the turbulent structure, visualization methods have been developed formulated in terms of the invariants of the velocity gradient tensor  $\partial u_i / \partial x_j$  (Where the decomposition of velocity gradient can be made into isotropic, symmetric-deviatoric, and antisymmetric parts:  $\frac{\partial u_i}{\partial x_j} = \frac{1}{3} \delta_{ij} + S_{ij} + \Omega_{ij}$ ). The  $Q$  criterion locates regions where rotation dominates over strain in the flow. Letting  $S_{ij}$  and  $\Omega_{ij}$  denote the symmetric and anti-symmetric parts of  $\frac{\partial u_i}{\partial x_j}$ , one defines  $Q$  as the second invariant of  $\frac{\partial u_i}{\partial x_j}$ , given as,

$$Q = \frac{1}{2} (\Omega_{ij}^2 - S_{ij}^2)$$

Where  $S_{ij}$  is the rate of strain tensor defined as  $S_{ij} = \frac{1}{2} \left( \frac{\partial u_i}{\partial x_j} + \frac{\partial u_j}{\partial x_i} \right)$  and  $\Omega_{ij} = \frac{1}{2} \left( \frac{\partial u_i}{\partial x_j} - \frac{\partial u_j}{\partial x_i} \right)$  is the rate of rotation tensor. A coherent vortex is defined as a region where  $Q > 0$ .

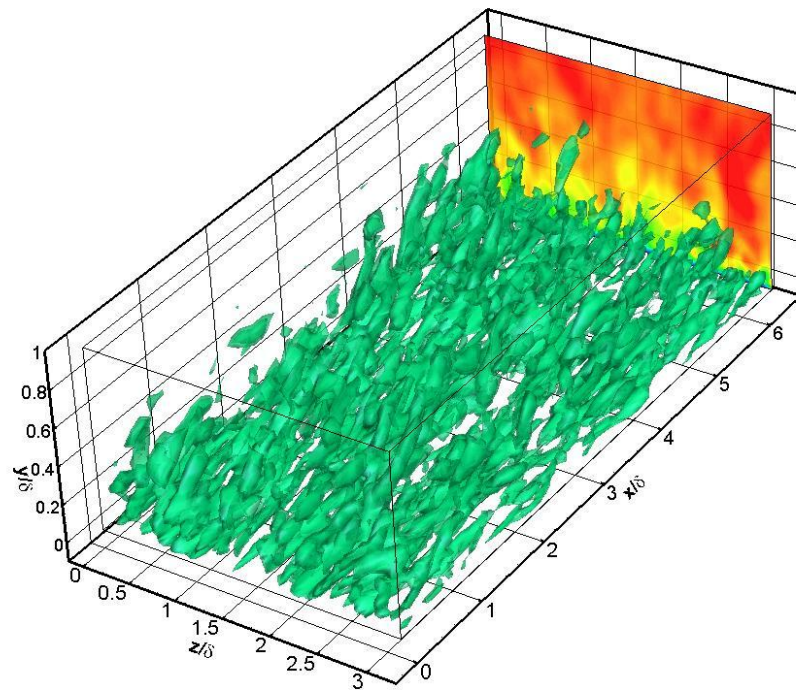
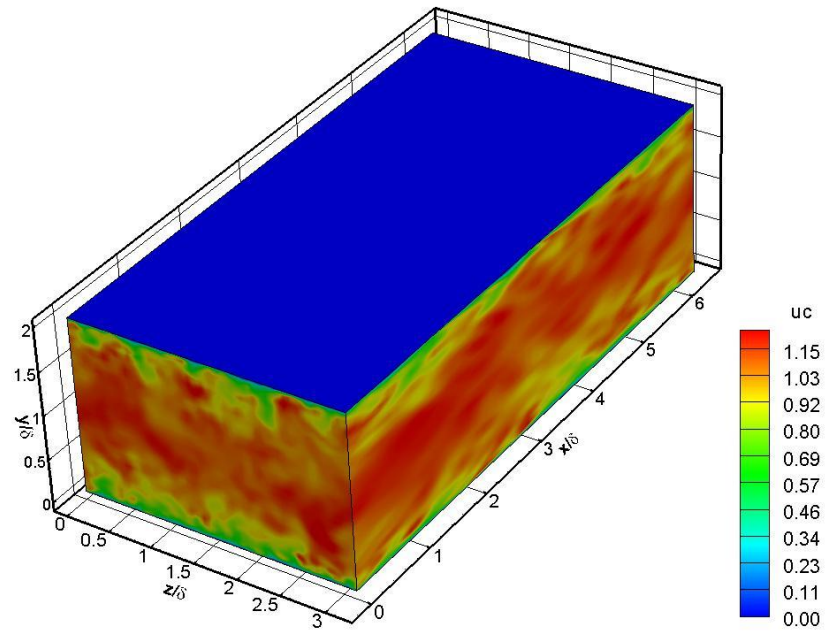


Figure 5.(a) Instantaneous three dimensional velocity contours (b) Turbulent eddy structure presented using Q-criterion visualization technique.

## 4.2 Turbulence in channel flow with variable properties

The objective of this section is to validate a turbulence study for the case where thermo-physical properties vary due to strong temperature gradients. This corresponds to a low-Mach number regime where compressibility effects can be neglected ( $M < 0.3$ ) and the effects of variable density based solely on temperature can be studied. Also, of interest is the response of the Large-eddy simulation model developments in complex cases where large variations in temperature, density and turbulence are coupled.

### 4.1.1 Wall bounded terminology and resolution requirements

The configuration used in this section corresponds to a planar channel with isothermal walls at different temperatures. In this case the lower wall (designated cold wall) is specified at  $T_1 = 300K$  and the upper wall (designated hot wall) is prescribed at  $T_2 = 600K$ . A classical Suntherland's law for viscosity is used where  $\nu \propto f(T)$  is used based on the reference temperature at the cold wall. In this way, the bulk Reynolds number is defined as  $Re_{bulk} = \frac{u_{bulk}\rho_{cold}\delta}{\mu_{cold}}$  where the bulk velocity is  $u_{bulk} = \frac{\int \rho(y)u(y)dy}{\int \rho(y)dy}$  (and is also a measure of the channel mass flux) and the values of density and dynamics viscosity correspond to the temperature at the cold wall. A skin friction coefficient,  $C_{f_i} = \frac{\tau_{wall_i}}{2\rho_i U^2}$ , is also used to characterize the flow at each wall where it is defined based on the mean density in the channel and maximum velocity. Using similar turbulent structure arguments, we define the relevant quantities for non-dimensionalization based on the viscosity, wall shear stress and heat flux. The opposing signs of temperature gradients at each wall indicate that the normalization of dependent variables in viscous units will be anti-symmetrical. The “thermal” viscous units for this case are defined

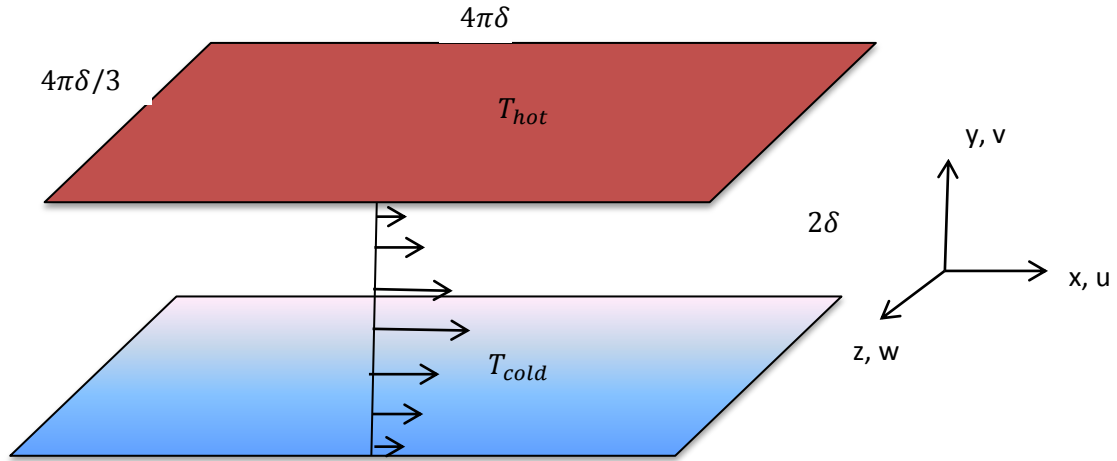
based on the frictional velocity  $u_{\tau_i} = \sqrt{\frac{\mu}{\rho_i} \frac{du}{dy}}_i$  and heat flux parameter  $B_{q_i} = \frac{-k_{wall} \frac{dT}{dy}|_i}{\rho_i c_p u_{\tau_i} T_{wall_i}}$  where the index  $i = 1, 2$  indicates the cold or hot wall. Thus the viscous wall units are described by use of the superscript  $^+$  as,

$$y_i^+ = \frac{y \rho_i \delta}{\mu_i}, \quad u_{\tau_i}^+ = \frac{u}{u_{\tau_i}}, \quad T_i^+ = \frac{(T_{wall_i} - T)}{B_{q_i} T_{wall_i}}$$

Where the viscous distance, velocity and temperature wall units are defined respectively.

## 4.2.2 Computational domain

The simulation is performed with periodic conditions applied in the homogenous directions, namely the streamwise (x) and spanwise (z) coordinates. Isothermal walls are specified through the use of Dirichlet boundary conditions prescribing the hot and cold wall boundaries and no-slip conditions specify the non-permeable kinematic wall condition. The pressure gradient is adjusted at every time step to impose a constant mass flux through the channel where the variations in density affect the description of the mass flux. The variable density turbulence models developed and implemented are the LES Dynamic Eddy Viscosity and Dynamic Eddy Diffusivity model with classical Smagorinsky type arguments used to describe the relationship between dynamics coefficients, shear stress and heat flux. An extension of the turbulent coefficient minimization scheme is used for the temperature scalars where Lagrangian averaging option suitable for complex (non-homogenous) flows is utilized. The computational periods and grid details were selected following the suggestion of Nicoud et al where the grid spacing in the streamwise and spanwise directions are respectively  $\Delta x^+ = 50$  and  $\Delta z^+ = 15$  in wall units.



$(L_x L_y L_z)^*$	$(n_x n_y n_z)$	<b>grid stretching</b>
$(4\pi\delta, 2\delta, 4\pi\delta/3)$	$(48, 65, 64)$	<ul style="list-style-type: none"> <li>- Wall-normal hyperbolic (<math>\alpha = 2.75</math>)</li> <li>- Uniform grid in <math>x, z</math></li> </ul>
<b>Resolution criteria</b> (finite differences)	<b>Turbulence model</b>	<b>Turbulent coefficient</b> Minimization technique (Lily, et al)
$\Delta x^+ \cong 50$ $\Delta z^+ \cong 15$ $y^+ \cong 1$	LES Dynamic eddy viscosity (Smagorinsky type model) $\tau_{ij}^r = -2\nu_t \bar{S}_{ij} = -2C_{ev} \Delta^2  \bar{S}_{ij}  \bar{S}_{ij}$	$C_{ev}(x, y, z, t) = -\frac{1}{2} \frac{\langle L_{ij} M_{ij} \rangle_{avg}}{\langle M_{ij} M_{ij} \rangle_{avg}}$ $C_\theta(x, y, z, t) = \frac{\langle K_j T_j \rangle_{avg}}{\langle T_j T_j \rangle_{avg}}$
$Re_{bulk} = 4300$	LES Dynamic eddy diffusivity $q_j = -\bar{\rho} C_\theta \frac{\partial \tilde{T}}{\partial x_j}$	<b>Averaging type:</b> Lagrangian Planar (option) Line (option)
<b>wall boundary</b>	<b>Mass flux option</b>	<b>Periodicity</b>
$u = v = w = 0$ $T_{cold} = 300K$ $T_{hot} = 600K$	Adjust pressure gradient to maintain constant mass flux	Streamwise, Spanwise